

Floquet-engineered pair and single-particle filters in the Fermi-Hubbard model

Friedrich Hübner¹, Christoph Dauer², Sebastian Eggert², Corinna Kollath¹ and Ameneh Sheikhan¹

¹Physikalisches Institut, University of Bonn, Nussallee 12, 53115 Bonn, Germany

²Department of Physics and Research Center OPTIMAS, Technische Universität Kaiserslautern, 67663 Kaiserslautern, Germany



(Received 9 December 2021; revised 3 August 2022; accepted 3 August 2022; published 5 October 2022)

We investigate the Fermi-Hubbard model with a Floquet-driven impurity in the form of a local time-oscillating potential. For strong attractive interactions a stable formation of pairs is observed. These pairs show a completely different transmission behavior than the transmission that is observed for the single unpaired particles. Whereas in the high-frequency limit the single particles show a maximum of the transition at low driving amplitudes, the pairs display a pronounced maximum transmission when the amplitude of the driving is close to the interaction amplitude U . We use the distinct transmission behavior to design filters for pairs or single particles, respectively. For example, one can totally block the transmission of single particles through the driven impurity and allow only for the transmission of pairs. We quantify the quality of the designed filters.

DOI: [10.1103/PhysRevA.106.043303](https://doi.org/10.1103/PhysRevA.106.043303)

I. INTRODUCTION

By the extended demand for the miniaturization of technical devices as transistors, nowadays a large effort is made in order to engineer quantum devices which work at the few-particle level. Previous work has been devoted in order to design filters separating quasiparticles with different properties. For example, quantum dot setups are commonly used as energy filters [1] and resonance phenomena in transport considering the interaction on the quantum dots were investigated [2–6].

Whereas in earlier studies mainly steady-state working principles have been investigated, during the past decade also the dynamic shaping and controlling of such devices attracted increasing attention. Progress in this field is rewarding since it opens the path to using the time-dependent complexity as a resource for novel states and tuning possibilities. For example, a periodic driving of the quantum dots has been realized [1]. However, the microscopic understanding of nonequilibrium situations of these quantum systems, in particular, in the presence of interaction remains a huge challenge.

One interesting and promising research direction in the past decade is dynamic driving of quantum systems with time-periodic fields in order to control their characteristic behavior [7,8]. A periodic drive has been applied in order to obtain the dynamical localization [9] and artificial magnetic fields [10–14] to phase transitions [15–20] or to control the bound pairs [21].

Theoretically, periodically modulated systems can be described using the so-called Floquet theory [8]. The time-periodic symmetry allows to solve the time-dependent Schrödinger equation in terms of an eigenvalue problem with a conserved quasienergy, analogous to the quasimomentum in Bloch's theorem. The Floquet solution corresponds to a stable steady state of the system and results in an effective Floquet Hamiltonian for the stroboscopic time evolution.

The topic of this paper is the interplay of a periodically driven impurity and interactions in quantum systems. Already on the single-particle level, some very interesting results for the transmission of time-periodic *local* fields have been obtained. One example is a periodically modulated quantum dot or quantum point contact which has been predicted to control the transmission of single particles through the dot [22,23] or through the quantum point contact [24]. Furthermore, a periodically modulated quantum dot has been proposed to induce bound states [25] or as a spin filter [26] for which one spin species is fully blocked whereas the other is fully transmitted by the dot.

As we show here, the effect of the interaction in combination with a time-periodic impurity field enhances the complexity considerably. In particular, for effective attractive interactions between fermionic particles as they occur in superconductors, we find that the formation of interaction-induced pairs leads to a highly nontrivial transmission behavior as a function of driving amplitude and frequency, which is very distinct from the single-particle behavior. This is a result of novel terms arising in this inhomogeneous system in an effective description by a Floquet-Schrieffer-Wolff transformation [27], not present in a homogeneous system by the interplay of the driving and the interaction. We show that the combination of interaction and nonequilibrium driving can indeed be used as a resource to construct novel devices, such as a pair filter or pair blocker.

II. MODEL AND EFFECTIVE DESCRIPTIONS

We consider a Fermi-Hubbard chain with a driven local potential at site 0 described by the Hamiltonian,

$$\begin{aligned} \mathbf{H}(t) = & -J \sum_{n,\sigma} (\mathbf{c}_{n\sigma}^\dagger \mathbf{c}_{n+1\sigma} + \text{H.c.}) + U \sum_n \mathbf{n}_{n\uparrow} \mathbf{n}_{n\downarrow} \\ & + \lambda\omega \cos(\omega t) (\mathbf{n}_{0\uparrow} + \mathbf{n}_{0\downarrow}). \end{aligned} \quad (1)$$

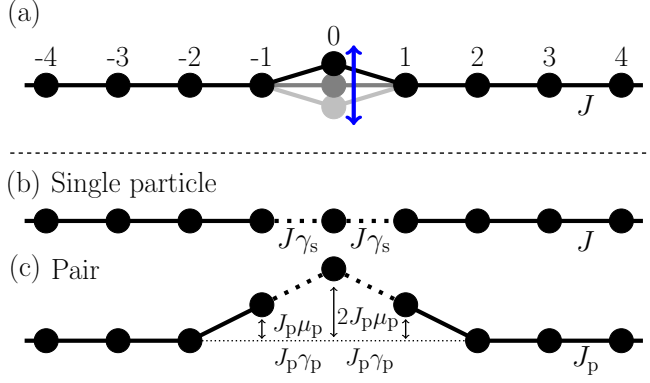


FIG. 1. (a) Sketch of the Fermi-Hubbard chain with a periodically driven potential at site 0. (b) and (c) Effective high-frequency models describing the scattering of a (b) single particle and a (c) pair, respectively. For the single particle and the pair the hopping to and from the impurity site (dashed line) is reduced by a factor of $\gamma_{s,p}$, respectively. For the pair, additionally, a triangular potential at sites $-1, 0$, and 1 arises.

Here the operator $\mathbf{c}_{n\sigma}^\dagger$ annihilates (creates) a fermion with spin $\sigma \in \{\uparrow, \downarrow\}$ on site n , $\mathbf{n}_{n\sigma} = \mathbf{c}_{n\sigma}^\dagger \mathbf{c}_{n\sigma}$ is the density operator, J is the hopping parameter, $U < 0$ is the attractive Hubbard interaction, and ω and λ are the frequency and dimensionless amplitude of the driving, respectively. Here, we set $\hbar = 1$ and measure the lengths in units of the lattice spacing. We will investigate the scattering of a single incoming particle or of an incoming on-site pair of spin-up and spin-down fermions at the impurity.

The scattering of a single particle at the periodically driven impurity has been studied in detail in Ref. [23]. At high driving frequencies $\omega \gg J$, an effective time-independent Floquet Hamiltonian can be derived using the high-frequency expansion [8,28]. Typically, the time evolution can be split into a so-called kick term and slow terms [7]. For the situation under consideration, it is specific that the time evolution of the effective model coincides with the time evolution of the original model after full periods of the driving [16]. For a single particle impinging on the periodically modulated impurity the effective Hamiltonian is given by

$$\begin{aligned} \mathbf{H}^s = & -J \sum_{n \neq -1,0} (\mathbf{c}_{n\uparrow}^\dagger \mathbf{c}_{n+1\uparrow} + \text{H.c.}) \\ & -JJ_0(\lambda) \sum_{n=-1,0} (\mathbf{c}_{n\uparrow}^\dagger \mathbf{c}_{n+1\uparrow} + \text{H.c.}), \end{aligned} \quad (2)$$

where J_0 is the Bessel function of the first kind. This effective model (see Fig. 1) describes a single particle on a chain with a reduced hopping amplitude from and to the impurity site 0. The effective hopping amplitude is reduced by the factor $\gamma_s = J_0(\lambda)$ which strongly depends on the driving amplitude λ . For a single particle with momentum k (in units of one over lattice spacing) the transmission through the impurity becomes $T_k^s = [1 + (\frac{1}{\gamma_s^2} - 1)^2 \cot^2 k]^{-1}$ [22]. Furthermore, the momentum-averaged transmission defined as $\bar{T} = \int_{-\pi}^{\pi} T_k \frac{dk}{2\pi}$, one can explicitly compute for a single particle giving $\bar{T}_s = \gamma_s^2 = J_0(\lambda)^2$. This means that the transmission of a single

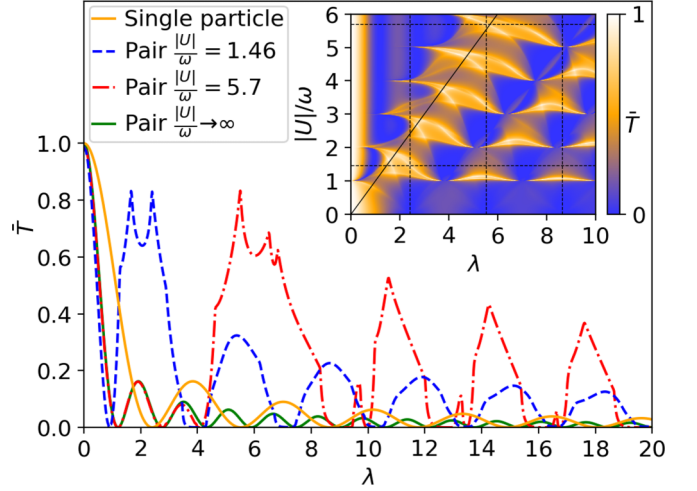


FIG. 2. Transmission in the limit $J \ll \omega, |U|$ as a function of the driving amplitude λ for a single particle (yellow line) and a pair at $|U|/\omega = 1.46$ (blue line), $|U|/\omega = 5.7$ (orange line), and $|U|/\omega \rightarrow \infty$ (green line). The inset shows the pair transmission versus λ and $|U|/\omega$. The vertical lines show the values of λ where the single-particle transmission vanishes. The horizontal lines show the values of $|U|/\omega$ which are shown in the main panel. The solid line shows $\lambda = |U|/\omega$ which is roughly the position of the first maximum.

particle (see Fig. 2) has a maximum at $\lambda = 0$, then strongly decays to its first zero at $\lambda \approx 2.4$. For larger values of λ an oscillating behavior is seen with a decaying amplitude. Therefore, the transmission of a single particle can be regulated by the amplitude of the driving. The analysis is not just limited to high frequencies in the single-particle case. Interesting resonances have been found at low driving frequencies in the momentum-resolved transmission using the full analysis of the noninteracting problem in Ref. [22]. The integrated transmission can be obtained in the adiabatic limit as an expansion for small $\lambda\omega$ to lowest order as $\bar{T}_s^{\text{low}} \approx 1 - \frac{\lambda\omega}{\pi J}$.

Let us now consider the intriguing effect of the interaction U . For strong attraction $-U \gg J, \omega$ using a Schrieffer-Wolff transformation the problem maps onto a model of stable entangled pairs which behave as noninteracting composite particles,

$$\mathbf{H}^{\text{eff}} = -J_p \sum_n (\eta_n^+ \eta_{n+1}^- + \text{H.c.}) + 2\lambda\omega \cos(\omega t) \eta_0^+ \eta_0^-,$$

where we defined the pair creation and annihilation operators $\eta_n^+ = \mathbf{c}_{n\uparrow}^\dagger \mathbf{c}_{n\downarrow}^\dagger$ and $\eta_n^- = \mathbf{c}_{n\downarrow} \mathbf{c}_{n\uparrow}$ and the effective pair hopping parameter $J_p = \frac{2J^2}{|U|}$. This effective Hamiltonian \mathbf{H}^{eff} clearly resembles the initial one Eq. (1) besides an effective tunneling amplitude J_p and driving amplitude 2λ of the impurity. Therefore, the scattering properties in the strong interacting limit can be derived from the known behavior for single particles. For example in the large frequency limit the pair transmission becomes $\bar{T}_p \approx J_0(2\lambda)^2$. Typically, due to the rescaled values, the single-particle transmission can still be evaluated in the low-frequency limit $\lambda\omega \ll J$ and $J < \omega$ where \bar{T}_s^{low} is valid, whereas for the pair transmission already the described high-frequency limit needs to be taken. This implies that if the

limit of large interaction is taken first, the pair transmission is typically much smaller than the single-particle transmission.

The most interesting and most complicated physical behavior occurs when the frequency is comparable to the interaction strength [29]. In order to tackle this case, we consider the limit $J \ll \omega, |U|$. It is indeed possible to have two leading energy scales and make a single rotation by using a Floquet-Schrieffer-Wolff transformation as described in Ref. [27] for homogeneous systems. In this inhomogeneous system this transformation leads to

$$\begin{aligned} \mathbf{H}^p = & -J_p \left[\sum_{n \neq -1, 0} (\eta_n^+ \eta_{n+1}^- + \text{H.c.}) \right. \\ & + \gamma_p \sum_{n=-1, 0} (\eta_n^+ \eta_{n+1}^- + \text{H.c.}) \\ & \left. + \mu_p (\eta_{-1}^+ \eta_{-1}^- + 2\eta_0^+ \eta_0^- + \eta_1^+ \eta_1^-) \right]. \end{aligned} \quad (3)$$

The periodic modulation of the impurity leads to the effective hopping amplitude and potential for the pair,

$$\gamma_p = \sum_{l=-\infty}^{\infty} \frac{\frac{|U|}{\omega} (-1)^l J_l(\lambda)^2}{\frac{|U|}{\omega} - l} \quad \text{and} \quad \mu_p = \sum_{l=-\infty}^{\infty} \frac{\frac{|U|}{\omega} J_l(\lambda)^2}{\frac{|U|}{\omega} - l} - 1,$$

respectively. Thus, within the effective Floquet description, the pair is subjected to a scattering at a region of three sites with scaled tunneling amplitude and a triangular potential (see Fig. 1). Let us comment that the effective potentials are only present in inhomogeneous systems.

III. TRANSMISSION

Using the effective model (3) we calculate in Appendix B that the momentum-dependent pair transmission through the impurity becomes

$$T_k^p = \frac{\gamma_p^4}{1 + \left(\frac{\varepsilon^p(k)}{\sin k}\right)^2 \left[\varepsilon^p(k)^2 - \gamma_p^2\right]^2 + \varepsilon^p(k)^2 \sin^2 k}, \quad (4)$$

with $\varepsilon^p(k) = \cos k - \mu_p$. We numerically integrate this expression in order to obtain the momentum-averaged transmission \bar{T}_p shown in Fig. 2. Its behavior is much more intriguing than the single-particle transmission, and the overall shape shows several pronounced features. (i) First, similar to the single-particle transmission for low driving amplitude the pair transmission is one (i.e., the system is fully transparent) at $\lambda = 0$ and decays quickly with increasing λ . (ii) Second, a remarkable feature is a pronounced maximum close to $\lambda \propto U/\omega$. Note that these maxima are a result of the interplay of all effective terms, in particular, the effective local potentials not present for the homogeneous system. (iii) For $\lambda > |U|/\omega$ the averaged transmission shows oscillations with decaying amplitude, giving alternating regions of high and low transmission. These features are crucial in order to design quantum filters, and we give a more detailed analysis of the origin of these features in the following. Let us comment that the nonanalytic behavior, which is not rare in scattering problems, seen in Fig. 2 is caused in this system by the contribution of the momenta around $k = 0, \pi$. Excluding the

surrounding area of these momenta in the integral leads to a smoothening of the cusps.

(i) The regime of small $\lambda \ll |U|/\omega$ can be understood by taking the limit $|U|/\omega \rightarrow \infty$ for which we obtain (see Ref. [30], Sec. 10.23) which gives $\gamma_p \rightarrow \sum_l (-1)^l J_l(\lambda)^2 = J_0(2\lambda)$ and $\mu_p \rightarrow \sum_l J_l(\lambda)^2 - 1 = 0$. This agrees with the results obtained from the large interaction limit described by \mathbf{H}^{eff} if additionally the large frequency limit is taken. We plot this result for $|U|/\omega \rightarrow \infty$ in Fig. 2 in red. It well approximates the initial decay of the transmission versus λ and provides a good approximation for $\lambda \ll |U|/\omega$.

(ii) For $\lambda \approx |U|/\omega$, a maximum occurs in the pair transmission. The maxima in the transmission occur if the relation $\pm\gamma_p + \cos k \sim \mu_p$ is approximately fulfilled. Due to the prefactor $\frac{1}{\frac{|U|}{\omega} - l}$ the expression for γ_p and μ_p are dominated by the Bessel function $J_{l_{\pm}}(\lambda)$ with l_{\pm} being the two integers closest to $\frac{|U|}{\omega}$. Both Bessel functions have their first maximum roughly around $\lambda \approx l_{\pm}$. At $\lambda \approx |U|/\omega$ they can, therefore, fulfill the relation which leads to the maxima of the pair transmission. Since we can tune the position of the maximum by tuning the value of the interaction, we will use it in order to design pair filters.

(iii) For $\lambda > |U|/\omega$ the transmission exhibits alternating regions of high and low transmission. The oscillations of the alternating regions roughly correspond to the oscillations of $J_{l_{\pm}}(\lambda)$. The detailed description of the amplitude of the transmission, however, requires taking into account more contributions. As λ increases the averaged pair transmission also decreases and vanishes in the limit $\lambda \rightarrow \infty$ since $\gamma_p \rightarrow 0$.

IV. PAIR FILTER

In the following we will use our gained understanding on the features of the single particle and pair transmissions in order to design filters. Here we concentrate on the momentum integrated transmission.

We start to design a pair filter, which should mainly transmit pairs through the impurity. We consider the quantity $r = \bar{T}_p(1 - \bar{T}_s)$. This measures the product of the transmission of pairs and the reflection of single particles at the impurity. Therefore, r gives the probability that the pair is transmitted whereas the single particle is reflected. The maximum value of r is $r = 1$ which corresponds to a perfect pair filter, i.e., only pairs can cross the impurity and these are transmitted with a probability equal one. The quantity r is plotted in Fig. 3 using the same values of $|U|/\omega$ as in Fig. 2.

For $\lambda \gtrsim 2$, r shows similarities to the pair transmission \bar{T}_p . In particular, the maxima for $\lambda \sim U/\omega$ and the oscillating structure of the additional local maxima persist. This behavior has its origin in the fact that for $\lambda > 2$ the single-particle transmission is small such that one can approximate $r \approx \bar{T}_p$. However, for $\lambda \lesssim 2$ the single-particle transmission typically gives an important contribution and reduces drastically the value of r . Therefore, the maxima of r for $\lambda \sim U/\omega$ for $\lambda \gtrsim 2$ are typically the optimal values for a pair filter. They often reach above the value of $r \gtrsim 0.8$ which constitutes already a good pair filter. If one requires additionally that the single particle is fully blocked, the most prominent values of λ for a pair filter are those were the single-particle transmission

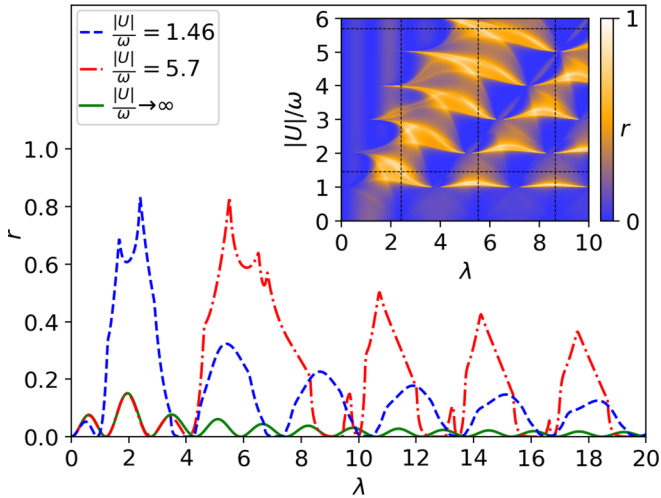


FIG. 3. Product of the transmission of pairs and the reflection of single particles at the impurity, $r = \bar{T}_p(1 - \bar{T}_s)$ versus the driving amplitude λ for $|U|/\omega = 1.46$ (blue), $|U|/\omega = 5.7$ (orange), and $|U|/\omega \rightarrow \infty$ (green). The inset shows r as function of λ and $|U|/\omega$. The vertical lines show the values of λ where the single-particle transmission vanishes. The horizontal lines show the values of $|U|/\omega$ which are shown in the main panel.

vanishes. This happens at the zeros of the Bessel function $J_0(\lambda)$, e.g., $\lambda \approx 2.4, 5.52, 8.65, \dots$. We mark these values in the insets of Figs. 2 and 3 as vertical lines. The values $|U|/\omega$ which we chose for the plots are optimal values for the first two zeros $\lambda \approx 2.4$ and $\lambda \approx 5.52$. For $|U|/\omega = 1.46$ the averaged pair transmission at $\lambda = 2.4$ is $\bar{T}_p = 0.79$ whereas for $|U|/\omega = 5.7$ at $\lambda = 5.52$ is $\bar{T}_p = 0.81$. This means that whereas the single particles are fully blocked also the pairs sometimes can get reflected, but with a low probability of about $\lesssim 0.2$. To summarize, we can design using the driven impurity good quality pair filters which mainly leave through pairs of particles.

In a similar fashion one can find configurations where the impurity acts as a single-particle filter, i.e., blocks most pairs and only transmits single particles. This can, in particular, be realized in the limit of large interaction (cf. \mathbf{H}^{eff}), a broad parameter regime exists where the single-particle transmission is described by the low-frequency expansion \bar{T}_s^{low} , whereas the pair transmission needs to be covered already in the high-frequency limit and takes the form of the squared Bessel function. Thus, in this parameter regime the single-particle transmission is always much larger than the pair transmission. Using even a driving value $2\lambda \approx 1.2$ leads to an almost vanishing pair transmission.

Tuning the amplitude of the driving λ and the ratio of U/ω further situations can be realized as, for example, a blocking of both single particles and pairs. We summarize the discussed configurations in Table I.

The effective model for the pair (3) is only applicable in the nonresonant case, where U is not an integer multiple of ω because both γ_p and μ_p diverge.

Let us point out that one of us also studied the resonant case [31], i.e., U/ω is an integer which goes beyond the scope of the current paper. A careful treatment of the pair breaking

TABLE I. Tunable impurity: A summary of parameter configurations yielding different filters.

$ U /\omega$	λ	\bar{T}_s	\bar{T}_p	Description
1.46	0.9	0.652	$< 10^{-3}$	Single-particle filter
	2.4	$< 10^{-3}$	0.794	Pair filter
5.7	1.2	0.45	$< 10^{-3}$	Single-particle filter
	2.64	0.013	0.006	Both blocked
	5.52	$< 10^{-3}$	0.81	Pair filter
∞	1.2	0.45	$< 10^{-3}$	Single-particle filter
	2.64	0.013	0.007	Both blocked

using the Lippmann-Schwinger equation shows that, as long as $J \ll \omega$, the resulting transmission is exactly given by the limiting expression of (4) [31]. In that sense Eq. (4) is valid for all parameters U/ω .

V. EFFECTS OF A BACKGROUND ON SINGLE-PARTICLE TRANSMISSION

Up to now we have focused on the situation of an incoming single particle or of an incoming pair of two particles in an otherwise empty system. In order to verify the stability of our results, we now consider an incoming particle on top of a noninteracting background. In Fig. 4 we show the density evolution in time for two different frequencies, $\omega = J$ which is within the bandwidth and $\omega = 40J$ which is much larger than the other energy scales of the system. The results are obtained using a time-dependent exact diagonalization method for a system of $L = 400$ sites. We find that the periodic driving of the impurity can induce considerable density oscillations, in particular, at low and intermediate driving frequencies. However, even though these oscillations are present, the transmission can be extracted by subtracting the densities of a system with and without incoming excitation. For very large frequencies the effect of driving on the background is mainly localized close to the impurity. As shown in Fig. 4 the extracted transmission from the nonperturbed background agrees well with the expected transmission for a single-particle T_k^s . This means that the transmission through the driven impurity seems stable also in the presence of a noninteracting background.

VI. CONCLUSION

To summarize we have designed a quantum device which can act as a filter for pairs and single particles. It consists of a periodically driven impurity in the chain of interacting fermions. Setting suitable driving parameters the driven impurity can be used to block incoming single particles or pairs. This, in particular, required taking carefully the limit of high frequency and interaction at the same time since otherwise the complex structure of Eq. (3) which leads to the interesting features does not occur. We identified optimal points of these filters. We further investigated the stability of the single-particle transmission against a noninteracting background. The study of the stability of the pair transmission to an interacting background is an open question which is not easy to tackle theoretically.

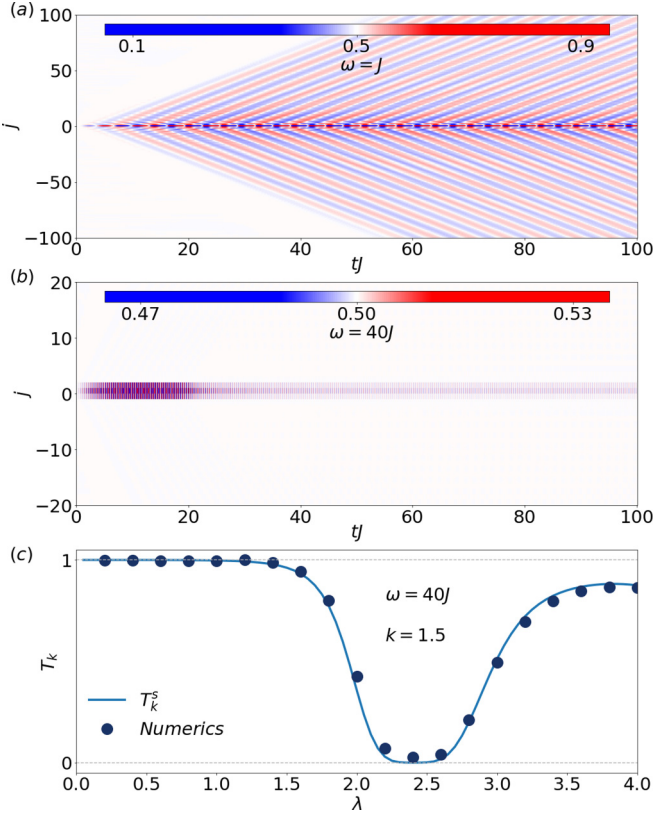


FIG. 4. Time evolution of the density for a chain of $L = 400$ sites with half-filled noninteracting fermions with the driven impurity at the central site with frequency (a) $\omega = J$ and (b) $\omega = 40J$. The driving amplitude is ramped up linearly up to the maximum value of $\lambda = 2.4$ in the ramp time $t_{\text{ramp}} = 20/J$. (c) The dependence of the single-particle transmission T_k on the driving amplitude λ . The driving frequency is $\omega = 40J$ and the incoming wave is a wave packet of a single hole with unitless momentum $k = 1.5$ and width $\sigma = 50$ sites in position space. The analytical result T_k^s (solid line) agrees well with the full numerical simulation (symbols).

One of the advantages of the Floquet-engineered impurity is that it does not only provide possible configurations for single-particle and pair filters but would also allow to quickly change between them in experiments by tuning, for example, the driving amplitude. Within this paper, we focused on the momentum-integrated transmission. Using the given equations, it can be easily used in order to design also momentum-dependent filters.

ACKNOWLEDGMENTS

We thank M. Köhl, H. Ott, and I. Schneider for stimulating discussions. We acknowledge funding from the Deutsche Forschungsgemeinschaft (DFG, German Research Foundation), in particular, under Projects No. 277625399-TRR 185 (A5,B3,B4) and No. 277146847-CRC 1238 (C05) and under Germany's Excellence Strategy-Cluster of Excellence Matter and Light for Quantum Computing (ML4Q) Grant No. EXC 2004/1-390534769 and the European Research Council (ERC) under the Horizon 2020 Research and Innovation programme, Grant Agreement No. 648166 (Phonton).

APPENDIX A: GAUGE TRANSFORMATION

In this Appendix we would like to explain how one derives a Fermi-Hubbard-like Hamiltonian with time-periodic hopping from (1) using the gauge transformation $\mathbf{U}(t) = e^{-i\lambda(\mathbf{n}_{0\uparrow} + \mathbf{n}_{0\downarrow}) \sin \omega t}$. For such a time-dependent gauge transformation the resulting Hamiltonian is given by

$$\mathbf{H}^g(t) = \mathbf{U}(t)^\dagger \mathbf{H}(t) \mathbf{U}(t) - i \text{div} t \mathbf{U}(t)^\dagger \dot{\mathbf{U}}(t). \quad (\text{A1})$$

The gauge transformation is defined as such that the last term exactly cancels the driving term in (1). It remains to compute the first part. To this end observe that

$$\mathbf{U}(t)^\dagger \mathbf{c}_{n\sigma} \mathbf{U}(t) = \begin{cases} e^{-i\lambda \sin \omega t} \mathbf{c}_{0\sigma}, & n = 0, \\ \mathbf{c}_{n\sigma}, & \text{else.} \end{cases} \quad (\text{A2})$$

By inserting $1 = \mathbf{U}(t)\mathbf{U}(t)^\dagger$ into Hamiltonian (1) one can use this result to compute the gauge transformation of all other quantities. For example,

$$\mathbf{U}(t)^\dagger \mathbf{c}_{n\sigma}^\dagger \mathbf{c}_{n+1\sigma} \mathbf{U}(t) = \begin{cases} e^{-i\lambda \sin \omega t} \mathbf{c}_{n\sigma}^\dagger \mathbf{c}_{n+1\sigma}, & n = -1, \\ e^{i\lambda \sin \omega t} \mathbf{c}_{n\sigma}^\dagger \mathbf{c}_{n+1\sigma}, & n = 0, \\ \mathbf{c}_{n\sigma}^\dagger \mathbf{c}_{n+1\sigma}, & \text{else,} \end{cases} \quad (\text{A3})$$

whereas any $\mathbf{c}_{n\sigma}^\dagger \mathbf{c}_{n\sigma}$ is unaffected by the gauge transformation.

We denote the prefactors in front of the hopping terms as $g_n(\omega t)$. Collecting all terms finally leads to

$$\mathbf{H}^g(t) = -J \sum_{n\sigma} [g_n(\omega t) \mathbf{c}_{n\sigma}^\dagger \mathbf{c}_{n+1\sigma} + \text{H.c.}] + U \sum_n \mathbf{n}_{n\uparrow} \mathbf{n}_{n\downarrow}, \quad (\text{A4})$$

where $g_n(\phi) = 1$ except for $g_{-1}(\phi) = e^{-i\lambda \sin(\phi)}$ and $g_0(\phi) = e^{i\lambda \sin(\phi)}$.

APPENDIX B: CALCULATION OF THE TRANSMISSION IN THE EFFECTIVE MODEL

Consider a pair coming from the left with momentum k and energy $\epsilon_k = -2J_p \cos k$. We would like to calculate the transmission amplitude. The wave function has the general form

$$\psi_n = \begin{cases} e^{ikn} + r_k e^{-ikn}, & n < 0, \\ \psi_0, & n = 0, \\ t_k e^{ikn}, & n > 0. \end{cases} \quad (\text{B1})$$

The Schrödinger equation evaluated at sites $n = -1, 0$, and 1 gives the following set of equations:

$$\psi_{-2} + \gamma_p \psi_0 + \mu_p \psi_{-1} = 2 \cos(k) \psi_{-1}, \quad (\text{B2})$$

$$\gamma_p \psi_{-1} + \gamma_p \psi_1 + 2\mu_p \psi_0 = 2 \cos(k) \psi_0, \quad (\text{B3})$$

$$\gamma_p \psi_0 + \psi_2 + \mu_p \psi_1 = 2 \cos(k) \psi_1. \quad (\text{B4})$$

Inserting the wave-function (B1) and solving the equations gives

$$t_k = \frac{\gamma_p^2}{1 - \mu_p e^{ik}} \frac{-2i \sin k}{(2, \cos k - 2\mu_p)(1 - \mu_p e^{ik}) - 2\gamma_p^2 e^{ik}}. \quad (\text{B5})$$

In order to obtain the transmission probability we have to square this expression $T_k = |t_k|^2$ which gives (4).

-
- [1] L. P. Kouwenhoven *et al.*, Mesoscopic electron transport, in *Proceedings of a NATO Advanced Study Institute*, edited by L. L. Sohn, L. P. Kouwenhoven, and G. Schön (Kluwer, Dordrecht, 1997), ser. E, Vol. 345, pp. 105–214.
- [2] M. Bylicki, W. Jaskólski, A. Stachów, and J. Diaz, *Phys. Rev. B* **72**, 075434 (2005).
- [3] E. Sela, H.-S. Sim, Y. Oreg, M. E. Raikh, and F. von Oppen, *Phys. Rev. Lett.* **100**, 056809 (2008).
- [4] A. V. Lebedev, G. B. Lesovik, and G. Blatter, *Phys. Rev. Lett.* **100**, 226805 (2008).
- [5] A. Nishino, T. Imamura, and N. Hatano, *Phys. Rev. Lett.* **102**, 146803 (2009).
- [6] D. Roy, A. Soori, D. Sen, and A. Dhar, *Phys. Rev. B* **80**, 075302 (2009).
- [7] N. Goldman and J. Dalibard, *Phys. Rev. X* **4**, 031027 (2014).
- [8] A. Eckardt and E. Anisimovas, *New J. Phys.* **17**, 093039 (2015).
- [9] H. Lignier, C. Sias, D. Ciampini, Y. Singh, A. Zenesini, O. Morsch, and E. Arimondo, *Phys. Rev. Lett.* **99**, 220403 (2007).
- [10] M. Aidelsburger, M. Atala, S. Nascimbéne, S. Trotzky, Y.-A. Chen, and I. Bloch, *Phys. Rev. Lett.* **107**, 255301 (2011).
- [11] C. Kollath, A. Sheikhan, S. Wolff, and F. Brennecke, *Phys. Rev. Lett.* **116**, 060401 (2016).
- [12] A. Sheikhan, F. Brennecke, and C. Kollath, *Phys. Rev. A* **93**, 043609 (2016).
- [13] A. Sheikhan, F. Brennecke, and C. Kollath, *Phys. Rev. A* **94**, 061603(R) (2016).
- [14] A. Sheikhan and C. Kollath, *Phys. Rev. A* **99**, 053611 (2019).
- [15] A. Zenesini, H. Lignier, D. Ciampini, O. Morsch, and E. Arimondo, *Phys. Rev. Lett.* **102**, 100403 (2009).
- [16] D. Poletti and C. Kollath, *Phys. Rev. A* **84**, 013615 (2011).
- [17] S. Kitamura and H. Aoki, *Phys. Rev. B* **94**, 174503 (2016).
- [18] S. Fazzini, P. Chudzinski, C. Dauer, I. Schneider, and S. Eggert, *Phys. Rev. Lett.* **126**, 243401 (2021).
- [19] T. Wang, S. Hu, S. Eggert, M. Fleischhauer, A. Pelster, and X. F. Zhang, *Phys. Rev. Res.* **2**, 013275 (2020).
- [20] A. Sheikhan and C. Kollath, *Phys. Rev. B* **102**, 035163 (2020).
- [21] K. Kudo, T. Boness, and T. S. Monteiro, *Phys. Rev. A* **80**, 063409 (2009).
- [22] S. A. Reyes, D. Thuberg, D. Pérez, C. Dauer, and S. Eggert, *New J. Phys.* **19**, 043029 (2017).
- [23] D. Thuberg, S. A. Reyes, and S. Eggert, *Phys. Rev. B* **93**, 180301(R) (2016).
- [24] O. Gamayun, A. Slobodeniuk, J.-S. Caux, and O. Lychkovskiy, *Phys. Rev. B* **103**, L041405 (2021).
- [25] A. Agarwala and D. Sen, *Phys. Rev. B* **96**, 104309 (2017).
- [26] D. Thuberg, E. Muñoz, S. Eggert, and S. A. Reyes, *Phys. Rev. Lett.* **119**, 267701 (2017).
- [27] M. Bukov, M. Kolodrubetz, and A. Polkovnikov, *Phys. Rev. Lett.* **116**, 125301 (2016).
- [28] K. Takegoshi, N. Miyazawa, K. Sharma, and P. K. Madhu, *J. Chem. Phys.* **142**, 134201 (2015).
- [29] If U is close to an integer multiple of ω the driving can break the pair into two single particles. A first approximation gives that in order to avoid pair breaking, that the distance of U/ω to the nearest integer should be below $4J/\omega$. Note, that this implies that the maximum possible value of J/ω is $J/\omega = 0.125$.
- [30] NIST Digital Library of Mathematical Functions, <http://dlmf.nist.gov/>, Release 1.1.2 of 2021-06-15, edited by F. W. J. Olver, A. B. Olde Daalhuis, D. W. Lozier, B. I. Schneider, R. F. Boisvert, C. W. Clark, B. R. Miller, B. V. Saunders, H. S. Cohl, and M. A. McClain.
- [31] F. Huebner (unpublished).